A 10-Year Study on the Characteristics of Thunderstorms in Belgium Based on Cloud-to-Ground Lightning Data

Dieter R. Poelman

Royal Meteorological Institute of Belgium, Brussels, Belgium

ABSTRACT

Temporal and spatial distributions of cloud-to-ground (CG) lightning in Belgium are analyzed. Based on data from the European Cooperation for Lightning Detection (EUCLID) network, spanning a period of 10 years between 2004 and 2013, mean CG flash densities vary between $0.3 \, \mathrm{km^{-2} \, yr^{-1}}$ in the west up to $2.4 \, \mathrm{km^{-2} \, yr^{-1}}$ toward the east of Belgium, with an average flash density of $0.7 \, \mathrm{km^{-2} \, yr^{-1}}$. The same behavior is found in terms of thunderstorm days and hours, where in the east most of the activity is observed, with a drop-off toward the coast. The majority of lightning activity takes place in the summer months between May and August, accounting for nearly 90% of the total activity. Furthermore, the thunderstorm season reaches its highest activity in July in terms of CG detections, while the diurnal cycle peaks between 1500 and 1600 UTC. A correlation is found between the estimated peak currents and altitude, with on average higher absolute peak currents at lower elevations and vice versa. In addition, a cell tracking algorithm is applied to the data to monitor the behavior of the individual cells. It is found that the lightning cells travel at an average speed of about $25 \, \mathrm{km \, h^{-1}}$, with a preferred northeasterly direction of movement. At last, CG flash rates are strongly related to the cell area.

1. Introduction

Electrification has always grasped the interest and fascination of people. Over decades now, continuous efforts have further improved our understanding of this natural phenomenon. Present-day advancements are driven by the possibility to tackle unsolved questions from different angles. This can be done for instance by performing high-voltage experiments in laboratories around the world, carrying out meteorological studies related to the initiation of lightning with respect to thunderstorm development, its effect on air chemistry, or by direct and/or remote observations using high-speed image processing and/or lightning location systems (LLS). The outcome is not only relevant from a pure scientific point of view, but is considered to be a valuable input as well for engineers wanting to protect electronic systems from the deleterious effects of lightning.

Lightning discharges are a combination of complex physical processes, radiating nearly throughout the full spectrum domain of electromagnetic fields, from the very low frequencies (VLF) up to the very high frequencies (VHF) and into the optical. Even X-ray emission has been frequently detected in association with rocket-triggered lightning (Dwyer et al. 2011). As such, different detection and localization techniques are best suited to handle particular radiation patterns linked to a certain process in the formation of a lightning discharge. For instance, present-day lightning mapping arrays (LMA), using time-of-arrival (TOA) at VHF frequencies, locate isolated pulses with a high degree of accuracy thanks to time measurements with nanosecond accuracy. Hence, detailed spatial and temporal mapping of the development of the lightning channel is possible in three dimensions within a limited radius of the networks' center (Krehbiel et al. 1999; Rison et al. 1999, 2000). On the other hand, VLF/LF frequencies are best suited to locate cloud-to-ground (CG) return strokes (RS), using either direction finding (DF) and/or TOA techniques over a more extended regional area, with baselines between sensors much larger than is required for LMA networks. In addition, a limited part of the pulses produced by cloud flashes can be detected as well in the VLF/LF range, albeit with considerable less location accuracy and detection capability as compared to

Corresponding author address: Dieter R. Poelman, Royal Meteorological Institute, Ringlaan 3 Avenue Circulaire, B-1180 Brussels, Belgium.
E-mail: dieter.poelman@meteo.be

LMA. At even larger scales, long-range and global lightning detection offer the possibility to cover regions exhibiting limited detection coverage otherwise, such as oceans, thanks to energy propagation in the Earth–ionosphere waveguide. Some of the networks that make use of these long-distance propagation characteristics include the World Wide Lightning Location Network (WWLLN; Jacobson et al. 2006), the Met Office Arrival Time Difference network (ATDnet; Keogh et al. 2006), and the Vaisala Global Lightning Dataset (GLD360; Said et al. 2010, 2011). Likewise, lightning mapping from space provides total lightning observations on a global scale, based on the observed optical pulse at 777.4 nm. Note, however, that in this case no distinction is made between intracloud (IC) and CG discharges. Such observations have been done since the mid-1990s with the Optical Transient Detector (OTD) and the Lightning Imaging Sensor (LIS) on board the *MicroLab-1* (now known as *Orbview-1*) and the Tropical Rainfall Measuring Mission (TRMM) satellites, respectively (Boccippio et al. 2000; Thomas et al. 2000). The future of spaceborne lightning detection is assured by the ongoing development of the Geostationary Lightning Mapper (GLM) and Lightning Imager (LI) on board the Geostationary Operational Environmental Satellite-R (GOES-R) and Meteosat Third Generation (MTG) satellites, respectively. Hence, it is clear that today's researchers have a range of possibilities at their disposal, and can choose the method that best suits their research purpose. For a more in-depth overview of the history and techniques used in modern LLS, the interested reader is referred to Cummins and Murphy (2009).

By now, most regional LLS provide information on the spatial and temporal stroke and flash incidence, polarity, and peak current. All of which can be used and is relevant in terms of lightning protection systems, as well as for weather forecasting and climatology applications. However, one must always keep in mind that observations of a network do not necessarily represent the absolute truth. Obviously, the performance of a network depends on the position and type of sensors, sensor outages, the method used to determine the ground strike locations, topographic effects, and so on. Hence, homogeneous performance over a large region is almost never reached.

Many climatology studies based on ground-based LLS already exist. The most well-documented LLS is that of the U.S. National Lightning Detection Network (NLDN), with numerous studies being published since its deployment in 1989 (e.g., Orville 1991, 2001; Orville and Silver 1997; Huffines and Orville 1999; Orville and Huffines 1999; Orville et al. 2002; Zajac and Rutledge 2001; Orville 2008). Many regional climatology studies

on the European continent exist as well (e.g., Finke and Hauf 1996; Schulz et al. 2005; Rivas Soriano et al. 2005; Antonescu and Burcea 2010, Tuomi and Mäkelä 2008; Santos et al. 2012; Mäkelä et al. 2014). Nevertheless, a thorough investigation into the lightning properties in Belgium has yet to be presented. To account for this lack of information, the CG lightning activity between 2004 and 2013 is analyzed in terms of its temporal and spatial occurrence over Belgium.

The lightning data used throughout this work are described in section 2. Treatment of the data to produce the temporal and spatial maps is included in section 3, as well as a description of the thunderstorm tracker used in the analysis. Section 4 is reserved to illustrate and interpret the results, while section 5 concludes with a summary.

2. Data

From 2001 onward several national meteorological services (NMS) and commercial companies within Europe joined forces to combine their respective operational LLS into the so-called European Cooperation for Lightning Detection (EUCLID). This is possible, since all of the individual sensors within the EUCLID network operate over the same LF frequency range. As such, the individual raw sensor data are sent in real time to a single central processor, calculating the electrical activity at any given moment. The use of a common central processor ensures that the resulting data are as consistent as possible throughout Europe, and is frequently of higher quality opposed to a simple composite of the individual LLS due to the implicit redundancy produced by shared sensor information. The location of EUCLID sensors in the neighborhood of Belgium are depicted in Fig. 1.

The performance of EUCLID has been frequently tested over the years in terms of its location accuracy (LA), detection efficiency (DE), and peak current estimation, made possible by comparing to direct lightning measurements at the Gaisberg tower (GBT) in Austria (Diendorfer et al. 2011) and/or to data obtained by a mobile video and electric field recording system (VFRS) taken at different locations (Schulz et al. 2014). Most recent validation efforts employing the VFRS took place at various locations in Austria from 2009 to 2012 (Schulz et al. 2012), in Belgium throughout August 2011 (Poelman et al. 2013), and during the Hydrological Cycle in Mediterranean Experiment (HYMEX) in southern France (Ducrocq et al. 2013) in 2012. Based on the ground truth campaign in Belgium, most relevant for this study, the median LA is 600 m, whereas the DE for negative strokes and flashes reaches 84% and 100%,
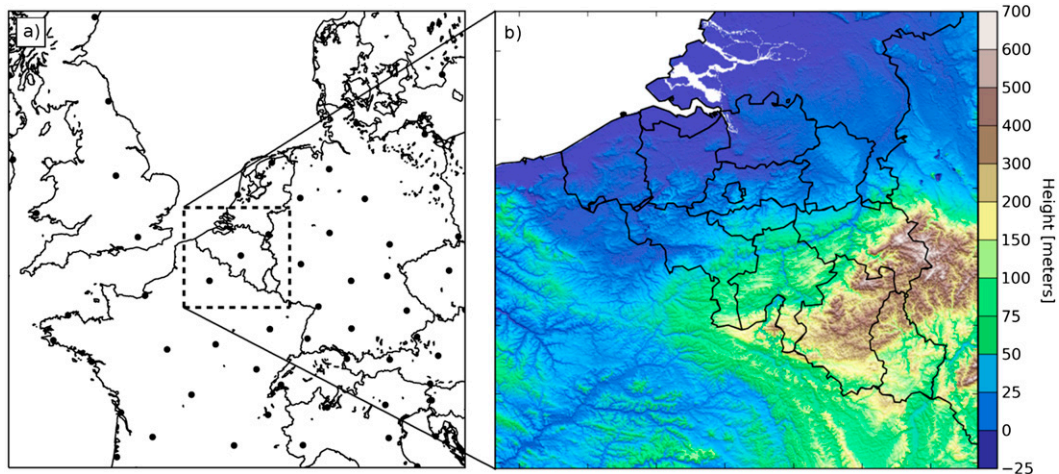
FIG. 1. (a) Location of some of the EUCLID sensors (dots) in and around Belgium at present and (b) the topography of Belgium.

respectively. Considering this excellent flash DE, no correction factor has been applied to the data in the course of the paper. Last but not least, the EUCLID peak current estimates have been compared to direct current measurements to the GBT, from which one can deduce that 80% of the absolute peak current deviations are below 3.8 kA.

Even though EUCLID is an evolving network expanding gradually its boundaries and the amount and type of sensors participating over the years, it can be assumed that from 2004 onward the performance of the network has been optimal within the region of interest covering Belgium. A year-by-year analysis of the semimajor axis of the 50% positional confidence ellipse (SMA) and the average number of sensors used (ANSU) in the calculation of a solution reveals that SMA decreases from 400 m in 2004 to 100 m in 2013 with a median value of 300 m, while ANSU remains nearly stable around 13 throughout the period. Hence, we opt to use CG flash data from 2004 to 2013 in this study within the domain restricted to latitude 40°–52°N and longitude 2°–7°E as indicated by the dashed line in Fig. 1. The topography within this area is plotted as well in this figure, illustrating the difference in altitude between the west and east of Belgium. An increase in height toward the southeast of Belgium is noticed up to a maximum elevation of about 700 m.

3. Methodology

Initial CG stroke data are grouped into flashes by the central processor based on a spatial and temporal clustering technique, with individual strokes belonging to a particular flash if $\Delta t < 1.5$ s and $\Delta r < 10$ km. In addition, a temporal interstroke criterion, $\Delta t_{\mathrm{interstroke}}$, of 0.5 s

is used as well. These grouping criteria overlap well with those used in other studies (e.g., Cummins et al. 1998; Kuk et al. 2011), except for the more relaxed time criterion, compared to a Δt of 1 s, which is traditionally used. Since occasionally flashes are observed with a duration exceeding 1 s (e.g., Poelman et al. 2013), the time criterion used in this work is justified. The position and peak current of the first RS are chosen as the position and peak current of the CG flash. Note that positive flashes with peak currents smaller than 10 kA are likely to be misclassified as CG flashes when in fact those are more likely to be of intracloud nature (Cummins et al. 1998; Wacker and Orville 1999a,b; Jerauld et al. 2005; Orville et al. 2002; Cummins et al. 2006; Biagi et al. 2007; Grant et al. 2012). Therefore, we opt to remove them from the dataset. Geographical plots are presented with a spatial resolution of 3×3 km², or it is explicitly stated otherwise. Note that this adopted grid size is larger than the assumed LA of EUCLID within Belgium and is, hence, appropriate for this study. Spatial distribution maps of, for example, the flash density or peak current are then obtained by summing the relevant parameter and dividing it by the amount of flashes observed per grid cell.

Besides the temporal and spatial analysis of the data, results on the characteristics of the individual thunderstorm cells are presented as well in terms of their speed, direction of movement, and flash rate. For these purposes, the Austrian Thunderstorm Nowcasting Tool (A-TNT) is applied to the EUCLID dataset to identify, monitor, and track distinct electrically active cells. A-TNT is a development of the Central Institute for Meteorology and Geodynamics (ZAMG) in Austria and primarily builds upon the principles of tracking and monitoring of electrically charged cells (ec-TRAM; Meyer et al. 2009, 2013a).
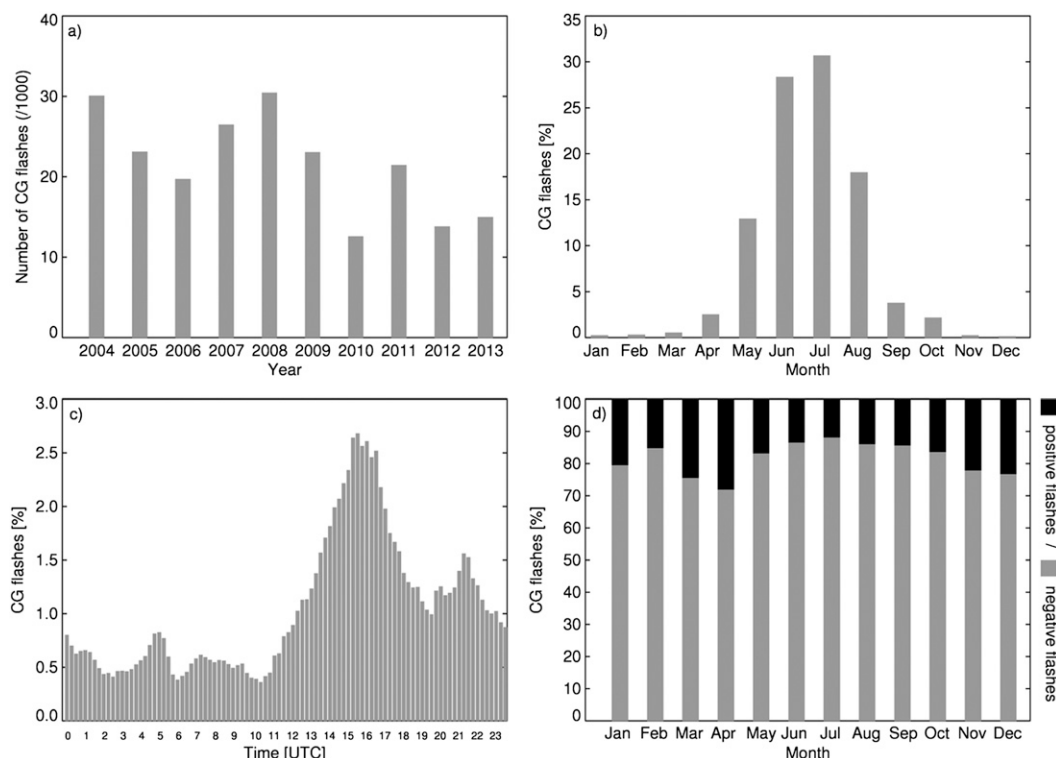
FIG. 2. (a) Annual cloud-to-ground flash counts, (b) mean monthly cloud-to-ground flash counts, (c) mean diurnal flash counts, and (d) mean monthly polarity distribution, based on 2004–13 EUCLID data.

In short, A-TNT ingests EUCLID flash data and subsequently identifies electrically active regions. The configuration parameters are set to a spatial resolution of $1 \times 1 \, km^2$. Every flash is then clustered to coherent areas by using a maximum search radius of 4 km. Lightning cells are generated every 3 min by mapping lightning data of the previous 3.5 min. These particular values have been selected to remain as close as where possible to the ones used in Meyer et al. (2013b), presenting results of total lightning thunderstorm tracking in south Germany, in order for the output to be compared. The incremental time step of 3 min limits the distance a particular cell traveled. Moreover, since the accumulation intervals overlap by 30 s, active lightning regions are supposed to overlap each other from one time step to the next in the accumulated data, allowing for a proper tracking of the cells. Individual cell parameters are generated and archived each time step and include the cell's area, number of flashes per cell, position, and an indicator for cell splitting and/or merging.

4. Results and analysis

a. Temporal statistics

Figure 2a displays the temporal distribution of the CG flash counts for the years 2004–13 within the Belgian borders. As expected, the number of CG flashes experiences a natural variability over the years, with an observed minimum of about 14 000 flashes in 2010 and increasing up to a maximum of approximately 30 000 flashes in 2008. Annual variations are found as well in other parts of the globe, and are attributed to the change in mesoscale and synoptic conditions influencing convective development of thunderstorms. Given the aforementioned behavior of SMA and ANSU, we believe these yearly variations in flash counts are not attributed to performance variations of the network. Note that it is not unlikely for a single day to dominate the total number of CG flashes detected during an entire thunderstorm season, especially over a region with the size of Belgium with an area of roughly 30 600 km².

The distribution of the mean monthly flash count is shown in Fig. 2b. It is found that nearly 90% of the electrical activity occurs during May–August, with a peak in July. On the other hand, the winter months account only for one percent of the observed lightning activity in Belgium, due to the different synoptic weather conditions compared to the summer months. This is expected since in Belgium solar radiation augments from April onward and reaches a maximum in July (Royal Meteorological Institute of Belgium 2014, personal communication). Consequently, the impinging solar

radiation heats the air near the ground, causing moist air masses to rise. This, in its turn, induces the onset of convective development. While this latter mechanism is almost absent during winter, storms during this season are mostly initiated by the movement of cold fronts.

In Fig. 2c the distribution of the diurnal flash count is indicated with a time resolution of 15 min and expressed in terms of percentage of the total CG flash activity. Note that in Belgium local time is UTC +1 and +2 h in winter and summer, respectively. A minimum is observed during the morning hours, accompanied by a steady increase from 1100 UTC onward up to the maximum point in the afternoon at about 1500–1600 UTC. This is then followed by a decrease in activity until the morning hours, interrupted by a second moderate peak around 2100 UTC. Such a secondary maximum has been observed as well by Finke and Hauf (1996) in southern Germany and is believed to be caused by long-lasting storms propagating from their southwesterly source areas in easterly direction. About 55% of the activity takes place between 1200 and 1900 UTC. The lower observed activity in the morning hours is inherent to the reduced occurrence of convective development due to solar heating of the ground and/or the atmospheric boundary layer, which begins at 1100 UTC. Nevertheless, a small peak is detected around 0500 UTC. An investigation into the cause of this peak reveals that it primarily stems from maximum one or two frontal thunderstorms per year. The overall diurnal behavior of CG flash counts overlaps well with those in surrounding countries in Europe (e.g., Finke and Hauf 1996; Schulz et al. 2005; Antonescu and Burcea 2010; Mäkelä et al. 2014) or for instance in Brazil (Pinto et al. 1999b).

Figure 2d shows the mean polarity distribution in Belgium for the individual months. Overall, 14% of the observed flashes are positive ones and this is slightly higher than what has been observed for instance in Austria (Schulz et al. 2005). The observed increase of positive flashes during the winter could be related to the decreased height of winter thunderstorms, lowering the upper positive charge of the cloud (Pinto et al. 1999a). The relative low percentage of positive flashes during January and February is believed to be an artifact of the low CG flash counts. Omitting January and February, this behavior is similar to other national reports in European countries (Schulz et al. 2005; Antonescu and Burcea 2010).

b. Spatial statistics

Figure 3a reveals the spatial distribution of the mean annual flash density N_g ($km^{-2} yr^{-1}$) derived from 215 000 CG flashes. Values range between 0.3 $km^{-2} yr^{-1}$ in the western part of Belgium and 2.5 $km^{-2} yr^{-1}$ located at the border between Belgium and Germany. The mean flash density is 0.7 $km^{-2} yr^{-1}$ and is in line with previous values based on the observations from an LLS employing Surveillance et Alerte Foudre par Interferometrie Radioelectrique (SAFIR) sensors (Poelman et al. 2012). It appears that the observed flash density in Belgium is rather moderate when compared to what is found in certain areas in the United States, Brazil, or other regions in the world with values easily exceeding the highest density in Belgium by a few factors or more, but is still considerably higher than what is generally observed in, for instance, northern Europe (Mäkelä et al. 2014). It is clearly visible that the spatial distribution follows the orography, with the highest values found in elevated terrain. This is not surprising since variations in the surrounding terrain are known to influence the onset of convection and thus the development of thunderstorms (Orville 1965; Kottmeier et al. 2008; Hagen et al. 2011; Cummins 2014). In the case of Belgium, evidence of the latter is further strengthened by the results as discussed at the end of this section, showing that the initiation of lightning cells is more likely to occur in regions with elevated terrain.

In Fig. 3b the spatial distribution of multiplicity of negative flashes in Belgium is plotted. The term multiplicity is used here to indicate the total number of strokes per flash and depends strongly on the stroke DE and adopted algorithm to group strokes into flashes. While the overall stroke DE of EUCLID is 84% in Belgium, this becomes 75% for strokes with absolute peak currents greater than 5 kA and increases to 90% for those with absolute peak currents over 15 kA (Poelman et al. 2013). A mean multiplicity of 2.1 and 1.3 for negative and positive flashes are found, respectively. The latter is in line with the values found from other LLS (Schulz et al. 2005), but is an underestimation when compared to ground truth recordings. For instance, based on ground truth recordings in Belgium, Poelman et al. (2013) found a mean multiplicity for negative flashes of 3.7, while similar multiplicities are found in comparable ground truth studies at different regions (e.g., Schulz et al. 2010; Saba et al. 2006; Rakov and Uman 1990). Of the negative flashes, 55% are single stroke flashes, whereas this value increases to 83% in case of positive flashes. Likewise, the high percentage of single stroke negative flashes is an overestimation with respect to ground truth observations, reporting in general values between 20% and 40% (Fleenor et al. 2009; Biagi et al. 2007; Poelman et al. 2013). One flash has been observed with a maximum multiplicity of 25, often related to upward lightning. Although some local variations are visible exhibiting higher multiplicity values in Fig. 3b, no clear trend is noticeable favoring one area with increased multiplicity compared to another.
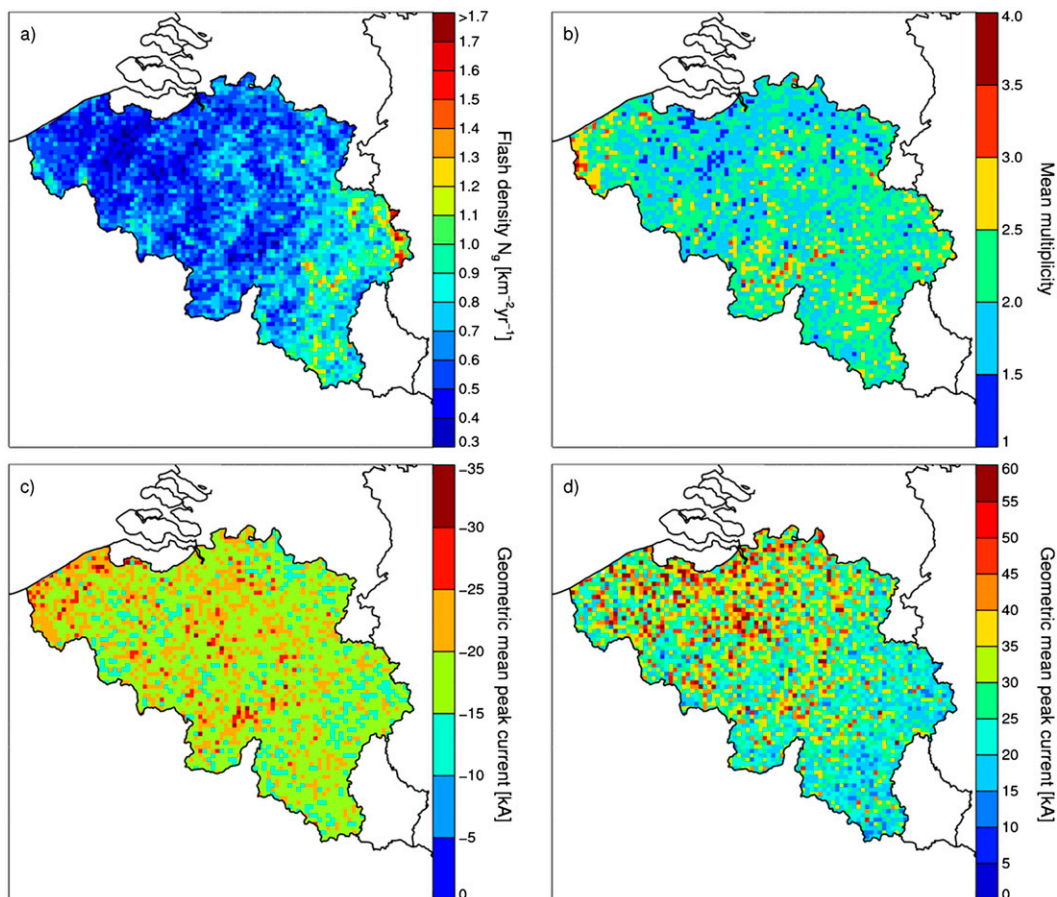
FIG. 3. Spatial distribution of (a) mean annual flash density ($km^{-2} yr^{-1}$), (b) multiplicity of negative flashes, (c) arithmetic mean peak current (kA) from first strokes in negative, and (d) in positive flashes, based on 2004–13 EUCLID data.

Figures 3c and 3d display the distribution of the arithmetic mean of estimated peak current magnitudes in negative and positive flashes, respectively. Mean (median) peak currents are -18 (-13) kA and $+33$ ($+21$) kA for negative and positive flashes, respectively. Besides the fact that in general positive RS tend to have higher absolute peak currents compared to negative RS, the relative high mean and/or median peak currents for positive flashes could be slightly influenced by the cutoff at 10 kA as well. In any case, the latter reported values agree fairly well with those reported by other LLS (e.g., Pinto et al. 1999a; Antonescu and Burcea 2010). One notices that toward the coastal region, the overall absolute flash amplitude increases, with a slight tendency of lower amplitude discharges in the southeast of Belgium, indicating a link between peak current and topography. Assuming a constant height of the bottom of clouds, an enhanced electric field between the cloud and terrain is induced with increasing altitude, facilitating the onset of discharges confined to regions of the cloud

with smaller quantities of charge as would be the case otherwise. This trend is quantified in Fig. 4, in which as a function of height, and binning in 50-m altitude steps, the mean peak current for negative and positive flashes is plotted. At sea level, the mean negative peak current for flashes is about -19 kA and this decreases to -16 kA for heights between 650 and 700 m. On the other side, for positive flashes the mean peak current decreases from 33 kA at sea level toward 20 kA for the highest regions in Belgium. However, the large variation in peak currents per altitude results in major standard deviation values, as plotted in the case for the negative peak currents. Nevertheless, Fig. 4 displays some dependency between altitude and peak current, even for the limited range of altitudes present within Belgium. This dependency between peak current and altitude has been demonstrated previously in Brazil by Pinto et al. (1999a) as well, with a clear change in the estimated peak currents around 1000 m.

Based on the individual CG detections in the 10-yr dataset, the related spatial distributions in terms of
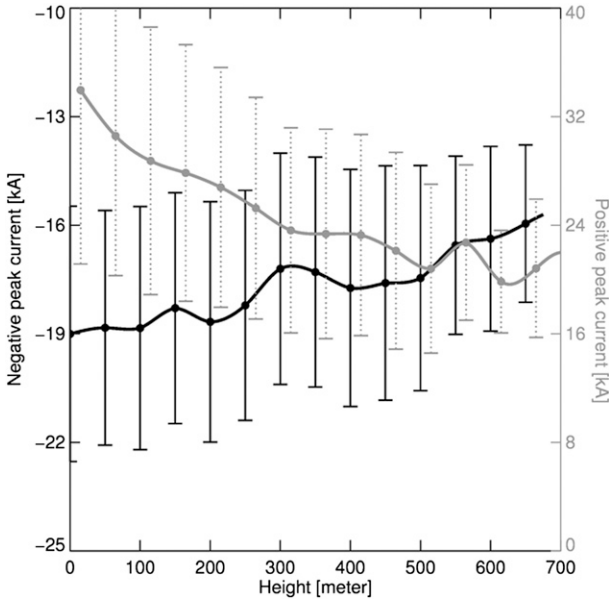
FIG. 4. Distribution of the mean peak current of negative (black) and positive (gray) flashes as a function of height in steps of 50 m in Belgium. In addition, the ±1 standard deviation is plotted as well.

observed during a day and/or hour. If this is the case, then T_d and/or T_h increase by one. We find that T_d varies between 8 and 21 days in Belgium, with an average of 16 storm days per year. The majority of thunderstorm days are located in the east of Belgium and drops off toward the west. Not surprisingly, the spatial pattern of T_d resembles the one found for N_g in Fig. 3a. The same behavior is found for T_h, with values ranking between 14 and 38 h, with an average of 26 h of lightning activity averaged over 10 years. Note that with a larger (lower) adopted sound travel radius T_d and T_h will increase (decrease) accordingly.

c. Cell tracking

In the following, the characteristics of the individual cells are further explored in more detail. A better knowledge of the properties of thunderstorm cells not only gives more insight into the physics of such systems, but can be beneficial for instance for nowcasting or lightning protection purposes. As mentioned earlier, A-TNT is applied to the EUCLID dataset within the domain restricted to latitude 49°–52°N and longitude 2°–7°E, as depicted in Fig. 1. For the analysis, we have chosen to extract solely those cells with a minimum lifetime of 15 min and which are neither truncated by the domain margins nor originating from cell splitting or disappearing in a cell merging process. As a result, a total of 6585 complete cell tracks and 46 000 individual cell entries are used in the analysis, bringing the mean lifetime of the cells up to about 21 min, comparable to the mean lifetime of the cells in Meyer et al. (2013b). The number of individual cell entries as a function of area is depicted in Fig. 6a. It is seen that the cells' area peaks between 65 and 110 km^2, with a mean and median area of 140 and 95 km^2, respectively. The distribution of

thunderstorm days T_d and hours T_h are plotted in Fig. 5. Here T_d and T_h can be considered as robust representations of the actual lightning activity. This is true since it tends to normalize the temporal variations in flash DE that might be present in the data (Bourscheidt et al. 2012). Bourscheidt et al. (2012) conducted a comparison of T_d obtained through human observations and LLS data. They found that the least-biased agreement between the two datasets was found when selecting a radius of 8 km. Therefore, T_d and T_h presented in this study are obtained by looking in a radius of 8 km around each grid cell centroid whether lightning has been
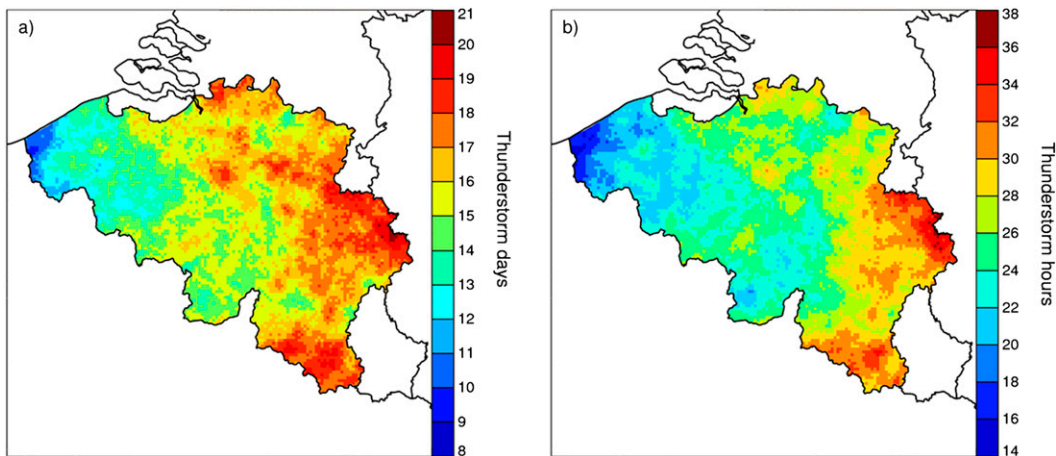

FIG. 5. Spatial distribution of mean thunderstorm (a) days and (b) hours per year, based on 2004–13 EUCLID data and adopting a sound travel radius of 8 km.
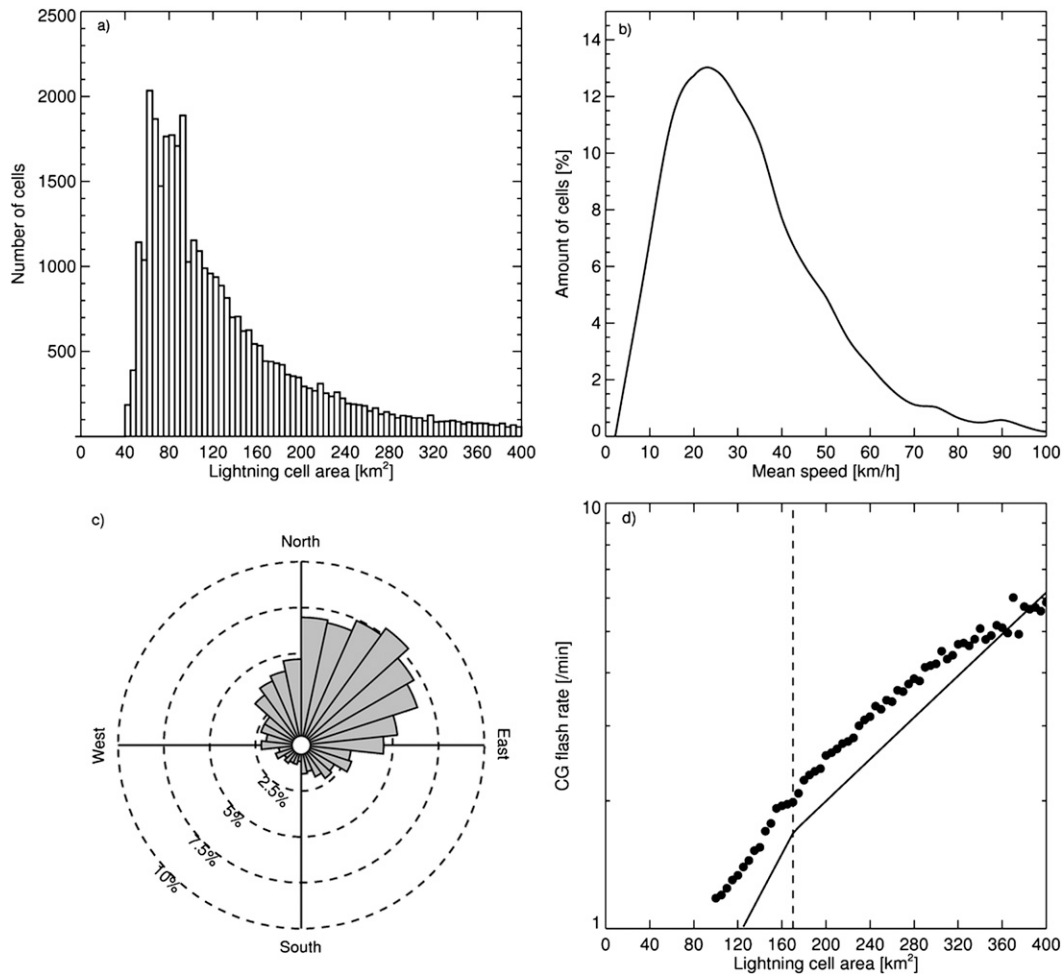
FIG. 6. (a) Number statistics of cell entries used for the analysis presented in (b)–(d). (b) Mean speed of cells. (c) Mean direction of cells. (d) Mean number of cloud-to-ground flash rates per lightning cell on logarithmic scale averaged over 5 km^2 cell area intervals based on EUCLID data (dots). In addition, the respective correlation function (solid line) from Meyer et al. (2013b) is added for comparison purposes.

the mean speed of the cells is visualized in Fig. 6b. The mean speed rises sharply and peaks around 25 km h^{-1}, followed by a steady drop toward higher values. A mean and median velocity of 31 and 27 km h^{-1} is found, respectively. Only 10% of the cells have velocities exceeding 50 km h^{-1}.

Figure 6c illustrates the distribution of the storm cells' direction averaged over 12° intervals. It is computed using the direction of movement between the first and last recorded position of the cell within the dedicated domain. A northeast direction is favored and is in agreement with the dominant wind direction during convective situations over Belgium. It is worth noting that the distributions of velocity and movement of direction found in this study overlap well with the results presented in Goudenhoofdt and Delobbe (2013), investigating the convective storm characteristics in

Belgium from volumetric weather radar observations spanning a 10-yr period with the use of the Thunderstorm Identification, Tracking, Analysis, and Nowcasting (TITAN) tool. They reported a prevalence of the northeast direction of movement of the storms, with about half of the storm tracks exhibiting speeds below 30 km h^{-1}, with a probability of only 5% to exceed 60 km h^{-1}.

Figure 6d plots the flash rate per cell on logarithmic scale normalized to 1-min intervals as a function of cell area, based on the CG flashes of EUCLID (dots). In addition, the statistical correlation function of CG flashes as presented in Meyer et al. (2013b) is plotted as a solid line. The latter is retrieved after applying a thunderstorm tracker onto stroke lightning location data over a region in south Germany. Stroke correlation functions were retrieved and subsequently transformed
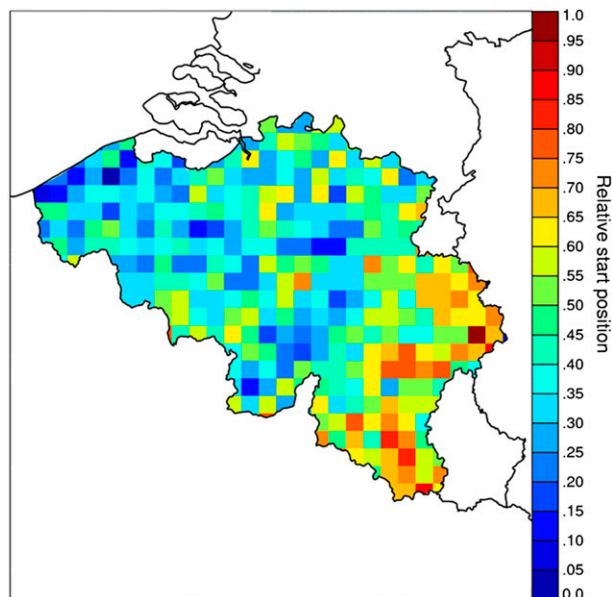
FIG. 7. Variation of the relative start position of convective cells within Belgium, adopting a spatial resolution of $10 \times 10\,km^2$.

into flash correlation functions. They noticed a break at $170\,km^2$ in the discharge characteristics, marking the point where storms develop into more complex structures. The flash rates per minute in this study follow closely the ones in Meyer et al. (2013b).

Based upon the cell entries, a density distribution plot of the start positions can be computed. This is done in Fig. 7, with values ranging from zero to one, adopting a spatial resolution of $10 \times 10\,km^2$. The maximum value is attributed to the location where most of the storms originate. It appears that the distribution of the initiation of convective storms follows the same pattern as N_g in Fig. 3a, with increased values toward the southeast of Belgium. Hence, orography can be accounted for this observed pattern.

5. Summary

Because of the variable nature of lightning occurrence from year to year, reliable insights into the lightning activity and parameters can only be achieved when based on large amounts of data. In this work, a total of 215 000 CG flashes recorded between 2004 and 2013 are used to analyze the spatial and temporal characteristics in Belgium. In addition, a thunderstorm tracker is applied to the EUCLID lightning dataset to examine some of the dynamic and physical properties of the electrified cells.

It is found that the lightning activity primarily takes place during the summer months between May and August, accounting for about 90% of the total observed lightning activity in Belgium. The thunderstorm season reaches its

peaks in July. This is not surprising since solar heating of the ground, being the driving force of convective development, is most intense during this period. Moreover, the percentage of positive CG flashes decreases during the summer. As regards the diurnal flash counts, those are the lowest during the morning hours, followed by a continuous increase from 1100 up to 1500–1600 UTC. Afterward, a gradual drop brings the flash counts back to the observed level at dawn.

The topography of Belgium accounts for the spatial patterns observed in terms of flash density, peak current estimates, and thunderstorm days and/or hours. For instance, flash density enhancements are visible toward the east of Belgium for regions above 300 m in comparison with the lower-lying areas toward the center and the coast. In addition, the geographical spread of T_d and T_h mirrors the behavior of N_g, since the computations are based upon the CG detections and an assumed sound travel radius. On the contrary, it is found that higher elevations favor flashes with a reduced observed absolute peak current.

After applying a thunderstorm tracker to the lightning dataset, the characteristics of the individual cells are analyzed based on a total of 6585 complete cell tracks, or 46 000 individual cell entries. The mean speed of the lightning cells is about $25\,km\,h^{-1}$, while only a minority of those reaching velocities exceeding $50\,km\,h^{-1}$ or more. The lightning cells favor a northeast direction, in accordance with the leading wind direction over Belgium. Moreover, flash rates per minute as a function of cell area follow the behavior found previously in Meyer et al. (2013b), with an observed change in behavior for cells larger than $170\,km^2$.

REFERENCES

Antonescu, B., and S. Burcea, 2010: A cloud-to-ground lightning climatology for Romania. *Mon. Wea. Rev.,* **138,** 579–591, doi:10.1175/2009MWR2975.1.

Biagi, C. J., K. L. Cummins, K. E. Kehoe, and E. P. Krider, 2007: National Lightning Detection Network (NLDN) performance in southern Arizona, Texas, and Oklahoma in 2003–2004. *J. Geophys. Res.,* **112,** D05208, doi:10.1029/2006JD007341.

Boccippio, D. J., and Coauthors, 2000: The Optical Transient Detector (OTD): Instrument characteristics and cross-sensor validation. *J. Atmos. Oceanic Technol.,* **17,** 441–458, doi:10.1175/1520-0426(2000)017<0441:TOTDOI>2.0.CO;2.

Bourscheidt, V., K. L. Cummins, O. Pinto Jr., and K. P. Naccarato, 2012: Methods to overcome lightning location system performance limitations on spatial and temporal analysis: Brazilian case. *J. Atmos. Oceanic Technol.,* **29,** 1304–1311, doi:10.1175/JTECH-D-11-00213.1.

Cummins, K. L., 2014: Mapping the impact of terrain on lightning incidence and multiple ground contacts in cloud-to-ground flashes. *Proc. 15th Int. Conf. on Atmospheric Electricity,* Norman, OK, ICAE, 16 pp. [Available online at http://www.nssl.noaa.gov/users/mansell/icae2014/preprints/Cummins_68.pdf.]

——, and M. J. Murphy, 2009: An overview of lightning locating systems: History, techniques, and data uses, with an in-depth look at the U.S. NLDN. *IEEE Trans. Electromagn. Compat.,* **51** (3), 499–518, doi:10.1109/TEMC.2009.2023450.

——, ——, E. A. Bardo, W. L. Hiscox, R. B. Pyle, and A. E. Pifer, 1998: A combined TOA/MDF technology upgrade of the U.S. National Lightning Detection Network. *J. Geophys. Res.,* **103,** 9035–9044, doi:10.1029/98JD00153.

——, J. A. Cramer, C. Biagi, E. P. Krider, J. Jerauld, M. A. Uman, and V. A. Rakov, 2006: The U.S. National Lightning Detection Network: Post-upgrade status. *Second Conf. on Meteorological Applications of Lightning Data,* Atlanta, GA, Amer. Meteor. Soc., 6.1. [Available online at https://ams.confex.com/ams/Annual2006/techprogram/paper_105142.htm.]

Diendorfer, G., H. Zhou, and H. Pichler, 2011: Review of 10 years of lightning measurement at the Gaisberg Tower in Austria. *Proc. Third Int. Symp. on Winter Lightning,* Sapporo, Japan, ISWL, 6 pp.

Ducrocq, V., and Coauthors, 2013: HyMeX-SOP1: The field campaign dedicated to heavy precipitation and flash flooding in the northwestern Mediterranean. *Bull. Amer. Meteor. Soc.,* **95,** 1083–1100, doi:10.1175/BAMS-D-12-00244.1.

Dwyer, J. R., M. Schaal, H. K. Rassoul, M. A. Uman, D. M. Jordan, and D. Hill, 2011: High-speed X-ray images of triggered lightning dart leaders. *J. Geophys. Res.,* **116,** D20208, doi:10.1029/2011JD015973.

Finke, U., and T. Hauf, 1996: The characteristics of lightning occurrence in Southern Germany. *Beitr. Phys. Atmos.,* **69** (3), 361–374.

Fleenor, S. A., C. J. Biagi, K. L. Cummins, E. P. Krider, and X.-M. Shao, 2009: Characteristics of cloud-to-ground lightning in warm-season thunderstorms in the central Great Plains. *Atmos. Res.,* **91,** 333–352, doi:10.1016/j.atmosres.2008.08.011.

Goudenhoofdt, E., and L. Delobbe, 2013: Statistical characteristics of convective storms in Belgium derived from volumetric weather radar observations. *J. Appl. Meteor. Climatol.,* **52,** 918–934, doi:10.1175/JAMC-D-12-079.1.

Grant, M. D., K. J. Nixon, and I. R. Jandrell, 2012: Positive polarity: Missclassification between intracloud and cloud-to-ground discharges in the Southern African Lightning Detection Network. *Proc. 22nd Int. Lightning Detection Conf.,* Broomfield, CO, Vaisala, 5 pp. [Available online at http://www.vaisala.com/en/events/ildcilmc/Pages/ILDC-2012-archive.aspx.]

Hagen, M., J. van Baelen, and E. Richard, 2011: Influence of the wind profile on the initiation of convection in mountainous terrain. *Quart. J. Roy. Meteor. Soc.,* **137,** 224–235, doi:10.1002/qj.784.

Huffines, G. R., and R. E. Orville, 1999: Lightning ground flash density and thunderstorm duration in the continental United States: 1989–96. *J. Appl. Meteor.,* **38,** 1013–1019, doi:10.1175/1520-0450(1999)038<1013:LGFDAT>2.0.CO;2.

Jacobson, A. R., R. Holzworth, J. Harlin, R. Dowden, and E. Lay, 2006: Performance assessment of the World Wide Lightning Location Network (WWLLN), using the Los Alamos Sferic Array (LASA) as ground truth. *J. Atmos. Oceanic Technol.,* **23,** 1082–1092, doi:10.1175/JTECH1902.1.

Jerauld, J., V. A. Rakov, M. A. Uman, K. J. Rambo, D. M. Jordan, K. L. Cummins, and J. A. Cramer, 2005: An evaluation of the performance characteristics of the U.S. National Lightning Detection Network in Florida using rocket-triggered lightning. *J. Geophys. Res.,* **110,** D19106, doi:10.1029/2005JD005924.

Keogh, S. J., E. Hibbett, J. Nash, and J. Eyre, 2006: The Met Office Arrival Time Difference (ATD) system for thunderstorms detection and lightning location. Forecasting Research Tech. Rep. 488, 22 pp.

Kottmeier, C., and Coauthors, 2008: Mechanisms initiating deep convection over complex terrain during COPS. *Meteor. Z.,* **17,** 931–948, doi:10.1127/0941-2948/2008/0348.

Krehbiel, P. R., R. J. Thomas, W. Rison, T. Hamlin, J. Harlin, and M. Davis, 1999: Three-dimensional lightning mapping observations during MEAPRS in central Oklahoma. *Proc. 11th Int. Conf. on Atmospheric Electricity,* NASA Conf. Publ. 1999-209261, Guntersville, AL, NASA, 376–379.

Kuk, B. J., H. I. Kim, J. S. Ha, and H. K. Lee, 2011: Intercomparison study of cloud-to-ground lightning flashes observed by KARITLDS and KLDN at South Lorea. *J. Appl. Meteor. Climatol.,* **50,** 224–232, doi:10.1175/2010JAMC2493.1.

Mäkelä, A., S.-E. Enno, and J. Haapalainen, 2014: Nordic lightning information system: Thunderstorm climate of Northern Europe for the period 2002-2011. *Atmos. Res.,* **139,** 46–61, doi:10.1016/j.atmosres.2014.01.008.

Meyer, V., H. Höller, K. Schmidt, and H.-D. Betz, 2009: Temporal evolution of total lightning and radar parameters of thunderstorms in southern Germany and its benefit for nowcasting. *Proc. Fifth European Conf. on Severe Storms (ECSS),* Landshut, Germany, European Severe Storm Laboratory, 2 pp.

——, ——, and H.-D. Betz, 2013a: Automated thunderstorm tracking: Utilization of three-dimensional lightning and radar data. *Atmos. Chem. Phys.,* **13,** 5137–5150, doi:10.5194/acp-13-5137-2013.

——, ——, and ——, 2013b: The temporal evolution of three-dimensional lightning parameters and their suitability for thunderstorm tracking and nowcasting. *Atmos. Chem. Phys.,* **13,** 5151–5161, doi:10.5194/acp-13-5151-2013.

Orville, H. D., 1965: A photogrammetric study of the initiation of cumulus clouds over mountainous terrain. *J. Atmos. Sci.,* **22,** 700–709, doi:10.1175/1520-0469(1965)022<0700:APSOTI>2.0.CO;2.

Orville, R. E., 1991: Lightning ground flash density in the contiguous United States—1989. *Mon. Wea. Rev.,* **119,** 573–577, doi:10.1175/1520-0493(1991)119<0573:LGFDIT>2.0.CO;2.

——, 2001: Cloud-to-ground lightning in the United States: NLDN results in the first decade, 1989–98. *Mon. Wea. Rev.,* **129,** 1179–1193, doi:10.1175/1520-0493(2001)129<1179:CTGLIT>2.0.CO;2.

——, 2008: Development of the National Lightning Detection Network. *Bull. Amer. Meteor. Soc.,* **89,** 180–190, doi:10.1175/BAMS-89-2-180.

——, and A. C. Silver, 1997: Lightning ground flash density in the contiguous United States: 1992–95. *Mon. Wea. Rev.,* **125,** 631–638, doi:10.1175/1520-0493(1997)125<0631:LGFDIT>2.0.CO;2.

——, and G. R. Huffines, 1999: Lightning ground flash measurements over the contiguous United States: 1995–97. *Mon. Wea. Rev.,* **127,** 2693–2703, doi:10.1175/1520-0493(1999)127<2693:LGFMOT>2.0.CO;2.

——, G. Huffines, W. Burrows, R. Holle, and K. Cummins, 2002: The North American Lightning Detection Network (NLDN)—First results: 1998–2000. *Mon. Wea. Rev.,* **130,** 2098–2108, doi:10.1175/1520-0493(2002)130<2098:TNALDN>2.0.CO;2.

Pinto, I. R. C. A., O. Pinto Jr., R. M. L. Rocha, J. H. Diniz, A. M. Carvalho, and A. C. Filho, 1999b: Cloud-to-ground lightning in southeastern Brazil in 1993: 2. Time variations and flash characteristics. *J. Geophys. Res.,* **104,** 31 381–31 387, doi:10.1029/1999JD900799.

Pinto, O., Jr., I. R. C. A. Pinto, M. A. S. S. Gomes, I. Vitorello, A. L. Padilha, J. H. Diniz, A. M. Carvalho, and A. C. Filho, 1999a: Cloud-to-ground lightning in southeastern Brazil in 1993: 1. Geographical distribution. *J. Geophys. Res.,* **104,** 31 369–31 379, doi:10.1029/1999JD900800.

Poelman, D. R., L. Delobbe, M. Crabbé, and C. Bouquegneau, 2012: Lightning activity in Belgium during 2001–2011. *Proc. 31st Int. Conf. on Lightning Protection,* Vienna, Austria, ICLP, 5 pp.

——, W. Schulz, and C. Vergeiner, 2013: Performance characteristics of distinct lightning detection networks covering Belgium. *J. Atmos. Oceanic Technol.,* **30,** 942–951, doi:10.1175/JTECH-D-12-00162.1.

Rakov, V. A., and M. A. Uman, 1990: Long continuing current in negative lightning ground flashes. *J. Geophys. Res.,* **95,** 5455–5470, doi:10.1029/JD095iD05p05455.

Rison, W. R., R. Scott, R. J. Thomas, P. R. Krehbiel, T. Hamlin, and J. Harlin, 1999: 3-dimensional lightning and dual-polarization observations of thunderstorms in central New Mexico. *Proc. 11th Int. Conf. on Atmospheric Electricity,* NASA Conf. Publ. 1999-209261, Guntersville, AL, NASA, 432–435.

——, W. P. Krehbiel, R. Thomas, T. Hamlin, and J. Harlin, 2000: A time-of-arrival lightning mapping system with high time resolution. *Eos, Trans. Amer. Geophys. Union,* **81** (Fall Meeting Suppl.), Abstract A52C-01.

Saba, M. M. F., O. Pinto Jr., and M. G. Ballarotti, 2006: Relation between lightning return stroke peak current and following continuing current. *Geophys. Res. Lett.,* **33,** L23807, doi:10.1029/2006GL027455.

Said, R. K., U. S. Inan, and K. L. Cummins, 2010: Long-range lightning geolocation using a VLF radio atmospheric waveform bank. *J. Geophys. Res.,* **115,** D23108, doi:10.1029/2010JD013863.

——, M. J. Murphy, N. W. S. Demetriades, K. L. Cummins, and U. S. Inan, 2011: Methodology and performance estimates of the GLD360 lightning detection network. *Proc. 14th Int. Conf. on Atmospheric Electricity,* Rio de Janeiro, Brazil, ICAE, 4 pp.

Santos, J. A., M. A. Reis, J. Sousa, S. M. Leite, S. Correia, M. Janeira, and M. Fragoso, 2012: Cloud-to-ground lightning in Portugal: Patterns and dynamical forcing. *Nat. Hazards Earth Syst. Sci.,* **12,** 639–649, doi:10.5194/nhess-12-639-2012.

Schulz, W., K. Cummins, G. Diendorfer, and M. Dorninger, 2005: Cloud-to-ground lightning in Austria: A 10-year study using data from a lightning location system. *J. Geophys. Res.,* **110,** D09101, doi:10.1029/2004JD005332.

——, H. Pichler, and G. Diendorfer, 2010: Evaluation of 45 negative flashes based on E-field measurements, video data and lightning location data in Austria. *Proc. 30th Int. Conf. on Lightning Protection,* Cagliari, Italy, Power and Energy Society, 2011-1-1014.

——, C. Vergeiner, H. Pichler, G. Diendorfer, and K. Cummins, 2012: Location accuracy evaluation of the Austrian lightning locations system ALDIS. *Proc. 22nd Int. Lightning Detection Conf.,* Broomfield, CO, Vaisala, 5 pp.

——, D. Poelman, S. Pédeboy, C. Vergeiner, H. Pichler, G. Diendorfer, and S. Pack, 2014: Performance validation of the European Lightning Location System EUCLID. *Proc. Int. Colloquium on Lightning and Power Systems,* Lyon, France, CIGRE, 9 pp.

Rivas Soriano, L., F. de Pablo, and C. Tomas, 2005: Ten-year study of cloud-to-ground lightning activity in the Iberian Peninsula. *J. Atmos. Sol.-Terr. Phys.,* **67,** 1632–1639, doi:10.1016/j.jastp.2005.08.019.

Thomas, R. J., P. R. Krehbiel, W. Rison, T. Hamlin, D. J. Boccippio, S. J. Goodman, and H. J. Christian, 2000: Comparison of ground-based 3-dimensional lightning mapping observations with satellite-based LIS observations in Oklahoma. *Geophys. Res. Lett.,* **27,** 1703–1706, doi:10.1029/1999GL010845.

Tuomi, T. J., and A. Mäkelä, 2008: Thunderstorm climate of Finland 1998–2007. *Geophysica,* **44,** 67–80.

Wacker, R., and R. Orville, 1999a: Changes in measured lightning flash count and return stroke peak current after the 1994 U.S. National Lightning Detection Network upgrade: 1. Observations. *J. Geophys. Res.,* **104,** 2151–2157, doi:10.1029/1998JD200060.

——, and ——, 1999b: Changes in measured lightning flash count and return stroke peak current after the 1994 U.S. National Lightning Detection Network Upgrade: 2. Theory. *J. Geophys. Res.,* **104,** 2159–2162, doi:10.1029/1998JD200059.

Zajac, B. A., and S. A. Rutledge, 2001: Cloud-to-ground lightning activity in the contiguous United States from 1995 to 1999. *Mon. Wea. Rev.,* **129,** 999–1019, doi:10.1175/1520-0493(2001)129<0999:CTGLAI>2.0.CO;2.